

Quinoline-Tethered N-Heterocyclic Carbene Complexes of Rhodium and Iridium: Synthesis, Catalysis, and Electrochemical Properties

Hong Mei Peng, Richard D. Webster,* and Xingwei Li*

Division of Chemistry and Biological Chemistry, School of Physical and Mathematical Sciences, Nanyang Technological University, Singapore 637371

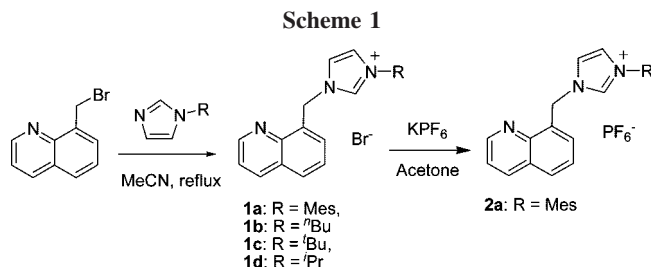
Received May 6, 2008

A series of rhodium and iridium complexes of quinoline-tethered hemilabile N-heterocyclic carbenes (NHC[^]N) have been synthesized via either deprotonation of imidazolium salts or silver transmetalation. Deprotonation of imidazolium ions by ^tBuOK in the presence of [Rh(COD)Cl]₂ (COD = 1,5-cyclooctadiene) afforded both chelating [Rh(COD)(NHC[^]N)]⁺ and monodentate [Rh(COD)(NHC)₂]⁺ complexes, while only the chelating carbene complexes were obtained for the iridium analogues. Silver transmetalation of this type of carbene to [M(COD)Cl]₂ (M = Rh, Ir) consistently afforded M(NHC)(COD)Cl, maintaining the metal chloride and pendant quinoline entity. Carbene transmetalation to (Cp^{*}IrCl)₂ gave an equilibrium mixture of neutral Cp^{*}Ir(NHC)Cl₂ and ionic [Cp^{*}Ir(NHC[^]N)Cl]Cl. All these rhodium and iridium cyclooctadiene complexes can undergo one-electron oxidation in cyclic voltammetry. The variable-scan-rate cyclic voltammetry experiments indicate that these compounds undergo slow heterogeneous electron transfer and that the oxidized forms are relatively short-lived. A neutral Rh(COD)(NHC)Cl complex proved to be active in catalyzing the [3 + 2] cycloaddition reactions of diphenylcyclopropenone and internal alkynes. Crystal structures of metal complexes in each category have been reported.

Introduction

Since the isolation of imidazole-based carbenes in the free state in 1991,¹ the significance of N-heterocyclic carbenes (NHCs) as ligands has been widely recognized and extensively reviewed.² In comparison to phosphine ligands, NHCs are stronger σ donors with tunable electronic and steric effects and their complexes are more robust,³ which are desirable features in catalysis. Transition-metal NHC complexes are particularly useful catalysts for organic transformations, and many of them have shown activity and stability higher than those of related phosphine complexes.⁴

Hemilabile NHC ligands featuring labile donors and an NHC moiety have the advantages of both the strongly binding NHC ligands and the more labile heteroatoms, since ligand lability is crucial for many efficient catalysts that rely on ligand



dissociation in the catalytic cycle.⁵ The chelation effect imparted to the metals can usually offer additionally desirable stability and activity. In the past several years, reported complexes with hemilabile NHC–N ligands include NHC–amine,⁶ NHC–imine,⁷ NHC–oxazoline,⁸ and NHC–pyridine systems.⁹ These systems have been mostly reported for palladium complexes that are highly useful catalysts for C–C cross-

* To whom correspondence should be addressed. E-mail: xingwei@ntu.edu.sg (X.L.); webster@ntu.edu.sg (R.D.W.).

(1) Arduengo, A. J., III; Harlow, R. L.; Kline, M. *J. Am. Chem. Soc.* **1991**, *113*, 361–363.

(2) (a) Herrmann, W. A. *Angew. Chem., Int. Ed.* **2002**, *41*, 1290–1309. (b) Nair, V.; Bindu, S.; Sreekumar, V. *Angew. Chem., Int. Ed.* **2004**, *43*, 5130–5135. (c) Arnold, P. L.; Pearson, S. *Coord. Chem. Rev.* **2007**, *251*, 596–609. (d) Sommer, W. J.; Weck, M. *Coord. Chem. Rev.* **2007**, *251*, 860–873. (e) Hahn, F. E.; Jahnke, M. C. *Angew. Chem., Int. Ed.* **2008**, *47*, 3122–3172.

(3) (a) Dorta, R.; Stevens, E. D.; Scott, N. M.; Costabile, C.; Cavallo, L.; Hoff, C. D.; Nolan, S. P. *J. Am. Chem. Soc.* **2005**, *127*, 2485–2495. (b) Kelly, R. A., III; Clavier, H.; Giudice, S.; Scott, N. M.; Stevens, E. D.; Bordner, J.; Samardjiev, I.; Hoff, C. D.; Cavallo, L.; Nolan, S. P. *Organometallics* **2008**, *27*, 202–210. (c) Dorta, R.; Stevens, E. D.; Hoff, C. D.; Nolan, S. P. *J. Am. Chem. Soc.* **2003**, *125*, 10490–10491.

(4) Kantchev, E. A. B.; O'Brien, C. J.; Organ, M. G. *Angew. Chem., Int. Ed.* **2007**, *46*, 2768–2813.

(5) (a) Jiménez, M. V.; Pérez-Torrente, J. J.; Bartolomé, M. I.; Gierz, V.; Lahoz, F. J.; Oro, L. A. *Organometallics* **2008**, *27*, 224–234. (b) Gade, L. H.; César, V.; Bellemin-Lapponnaz, S. *Angew. Chem., Int. Ed.* **2004**, *43*, 1014–1017. (c) César, V.; Bellemin-Lapponnaz, S.; Wadepohl, H.; Gade, L. H. *Chem. Eur. J.* **2005**, *11*, 2862–2873.

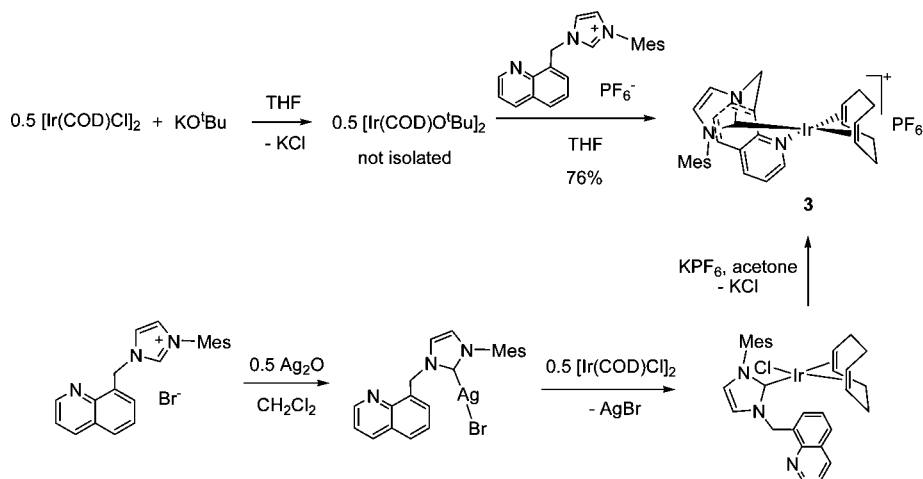
(6) (a) Houghton, J.; Dyson, G.; Douthwaite, R. E.; Whitwood, A. C.; Kariuki, B. M. *Dalton Trans.* **2007**, *28*, 3065–3073. (b) Anorld, P. L.; Mungur, S. A.; Blake, A. J.; Wilson, C. *Angew. Chem., Int. Ed.* **2003**, *42*, 5981–5984. (c) Douthwaite, R. E.; Houghton, J.; Kariuki, B. M. *Chem. Commun.* **2004**, 698–699.

(7) (a) Dastgir, S.; Coleman, K. S.; Cowley, A. R.; Green, M. L. H. *Organometallics* **2006**, *25*, 300–306. (b) Frøseth, M.; Dhindsa, A.; Røise, H.; Tilstet, M. *Dalton Trans.* **2007**, *23*, 4516–4524. (c) Coleman, K. S.; Chamberlayne, H. T.; Tuberville, S.; Green, M. L. H.; Cowley, A. R. *Dalton Trans.* **2003**, *23*, 2917–2922.

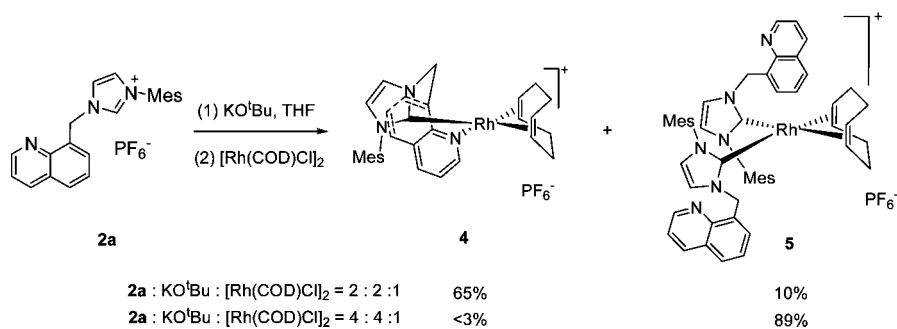
(8) (a) Perry, M. C.; Powell, M. T.; Cui, X.; Hou, D.-R.; Reibenspies, J. H.; Burgess, K. *J. Am. Chem. Soc.* **2003**, *125*, 113–123. (b) Poyatos, M.; Maise-Francois, A.; Bellemin-Lapponnaz, S.; Gade, L. H. *Organometallics* **2006**, *25*, 2634–2641. (c) Cesar, V.; Bellemin-Lapponnaz, S.; Gade, L. H. *Organometallics* **2002**, *21*, 5204–5208.

(9) (a) Danopoulos, A. A.; Tsoureas, N.; Macgregor, S. A.; Smith, C. *Organometallics* **2007**, *26*, 253–263. (b) Wang, X.; Liu, S.; Weng, L.-H.; Jin, G.-X. *Organometallics* **2006**, *25*, 3565–3569. (c) Gründemann, S.; Albrecht, M.; Kovacevic, A.; Faller, J. W.; Crabtree, R. H. *Dalton Trans.* **2002**, 2163–2167. (d) McGuinness, D. S.; Cavell, K. J. *Organometallics* **2000**, *19*, 741–748.

Scheme 2



Scheme 3



coupling or hydrosilylation reactions.^{8b,c} We now report the synthesis of a series of rhodium and iridium complexes with quinoline-functionalized NHCs (NHC⁺N), where the quinoline nitrogen may coordinate to metals under certain conditions. Importantly, Rh(COD)(NHC)Cl complexes can be employed as catalysts in the [3 + 2] cycloaddition reaction between diphenylcyclopropenone and alkynes. The carbene wingtip group has significant effects on the catalytic activity. Furthermore, some of these complexes have shown important electrochemical properties.

Results and Discussion

Preparation of Imidazolium Salts. Imidazolium salts **1a–d** were prepared from the quaternization of N-substituted imidazoles by 8-(bromomethyl)quinoline in MeCN under reflux (Scheme 1). The ¹H NMR spectra (CDCl₃) of compounds **1a–d** show that imidazolium C(2)–H characteristically resonates in the narrow range δ 10.40–10.88. The bromide anion in **1a** can be readily exchanged with PF₆[−] to give compound **2a**.

Iridium Cyclooctadiene Complexes. Irradiation of these carbenes was performed first via two general methods, starting from the corresponding imidazolium ions: direct metalation¹⁰ and silver transmetalation (Scheme 2).^{11,12a} In the direct metalation route, treatment of [Ir(COD)Cl]₂ with 2 equiv of ^tBuOK gave [Ir(COD)O^tBu]₂ in situ, which further reacted with imidazolium **2a** to afford chelating carbene complex **3** in 76% overall yield. We also noted that complex **3** could be obtained in similar yield when **2a** was first treated with ^tBuOK to generate the corresponding carbene in situ, followed by metalation with [Ir(COD)Cl]₂. Alternatively, a silver carbene complex was obtained when **1a** was stirred with Ag₂O (0.5 equiv) in CH₂Cl₂. Subsequent addition of [Ir(COD)Cl]₂ (0.5 equiv) afforded the

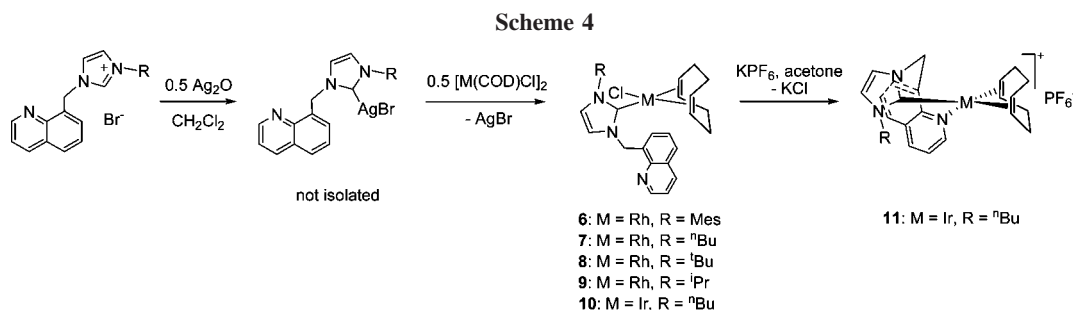
corresponding monodentate Ir(COD)(NHC)Cl complex, and chloride abstraction by KPF₆ eventually gave **3** in 94% yield.

Rhodium Cyclooctadiene Complexes. However, when we applied the direct metalation method to the synthesis of the rhodium analogue of **3**, we obtained both **4** and **5** in 65% and 10% yield, respectively (Scheme 3). The ¹H NMR spectrum of product **5** shows that the ratio of carbene to COD is 2:1, and the identity of product **5** was confirmed by X-ray crystallography and mass spectrometry. We reason that the yield of bis(carbene) **5** can be maximized by increasing the ratio of carbene to rhodium. Indeed, when we used **2a**, ^tBuOK, and [Rh(COD)Cl]₂ in a 4:4:1 ratio, the yield of **5** was improved to 89%, with essentially no mono(carbene) complex **4**. Here the difference between [Rh(COD)Cl]₂ and [Ir(COD)Cl]₂ in this direct metalation reaction likely originates from the strength of the M–N_{quinoline} bond (M = Ir, Rh). The quinoline N atom in complex **4** is more labile when it is bound to Rh and can be readily substituted by the second incoming NHC, while no such substitution took place

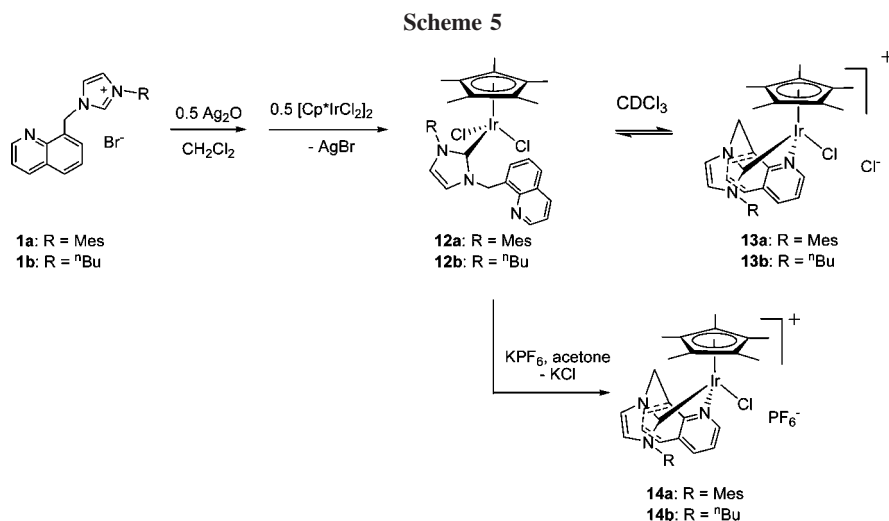
(10) (a) Jin, C.-M.; Twamley, B.; Shreeve, J. M. *Organometallics* **2005**, *24*, 3020–3023. (b) Baskakov, D.; Herrmann, W. A.; Herdtweck, E.; Hoffmann, S. D. *Organometallics* **2007**, *26*, 626–632. (c) Mata, J. A.; Poyatos, M.; Peris, E. *Coord. Chem. Rev.* **2007**, *251*, 841–859.

(11) (a) Mata, J. A.; Chianese, A. R.; Miecznikowski, J. R.; Poyatos, M.; Peris, E.; Faller, J. W.; Crabtree, R. H. *Organometallics* **2004**, *23*, 1253–1263. (b) Wanniarachchi, Y. A.; Khan, M. A.; Slaughter, L. M. *Organometallics* **2004**, *23*, 5881–5884.

(12) (a) Alcarazo, M.; Roseblade, S. J.; Cowley, A. R.; Fernandez, R.; Brown, J. M.; Lassaletta, J. M. *J. Am. Chem. Soc.* **2005**, *127*, 3290–3291. (b) Herrmann, W. A.; Fischer, J.; Ófele, K.; Artus, G. R. J. *J. Organomet. Chem.* **1997**, *530*, 259–262. (c) Herrmann, W. A.; Frey, G. D.; Herdtweck, E.; Steinbeck, E. *Adv. Synth. Catal.* **2007**, *349*, 1677–1691. (d) Huang, J.; Stevens, E. D.; Nolan, S. P. *Organometallics* **2000**, *19*, 1194–1197. (e) Martin, H. C.; James, N. H.; Aitken, J.; Gaunt, J. A.; Adams, H.; Haynes, A. *Organometallics* **2003**, *22*, 4451–4458. (f) Neveling, A.; Julius, G. R.; Cronje, S.; Esterhuysen, C.; Raubenheimer, H. G. *Dalton Trans.* **2005**, 181–192.

**Table 1. Selected NMR Signals (CDCl₃) of Iridium and Rhodium COD Complexes 3–11**

	3	4	5	6	7	8	9	10	11 ^a
CH ₂ (diastereotopic)	5.90/6.97	5.86/8.54	5.30/7.12	6.38/6.95	6.40/6.57	6.83/7.08	6.40/6.57	6.27/6.44	6.08/6.53
C _{carbene}	172.8	175.4	183.0	182.4	181.7	180.6	181.4	179.9	179.5

^a In CD₃CN.

for the iridium analogue. We also noted that it is relatively less common to have rhodium complexes of bis(carbene) in a monodentate mode.¹² As a contrast, iridium or rhodium cyclooctadiene complexes (**6–10**) obtained from silver transmetalation are consistently monodentate NHC complexes with a pendant quinoline moiety, from which chloride abstraction by KPF₆ can cleanly give the corresponding ionic chelating complexes (Scheme 4). The ¹H NMR spectrum (CDCl₃ or CD₃COCD₃) of complex **11** shows poorly resolved signals for virtually every peak, even at –40 °C. Those signals appear significantly improved in CD₃CN, although the CH₂ linker signal is still slightly broadened in comparison with that of the analogous complex **3**. In the ¹³C spectrum in CD₃CN, however, we can only observe one sharp peak (δ 83.7) and one broad peak (δ 53.1) for the COD olefinic CH groups, although four COD methylene signals are well-resolved. Furthermore, in the ¹³C NMR spectrum, in addition to the signal of free solvent CD₃CN (δ 1.32, septet), a new signal can be found (δ 1.20, septet) that is attributed to the coordinated CD₃CN. It is likely that the quinoline arm of the NHC–quinoline ligand is reversibly substituted by CD₃CN, which is probably the origin of the dynamic process responsible for signal broadening in ¹H and ¹³C NMR spectra.

All these iridium and rhodium cyclooctadiene complexes were characterized by NMR spectroscopy, and characteristic signals are given in Table 1. In the ¹H NMR spectra, all the linker CH₂ protons are diastereotopic, indicating that there is a hindered rotation along the M–C_{carbene} bond and complexes **3**, **4**, and **6–11** are all C₁ symmetrical. ¹H NMR spectra also show that

the differences in the chemical shifts of these two diastereotopic protons are more significant in chelating NHC⁺N complexes (**3** and **4**), possibly due to the endo and exo orientation of these two protons with respect to the seven-membered metallacycle. The carbene C atoms resonate characteristically in the range δ 172–183.

Iridium Cp* Complexes via Silver Transmetalation. We then applied silver transmetalation of this type of carbene to [Cp*IrCl₂]₂ to determine whether these NHCs can be chelating ligands in this different Ir(III) environment.¹³ Transmetalation readily took place from the silver carbene bromide complexes (Scheme 5). However, ¹H NMR spectroscopy shows two sets of peaks for the transmetalation products obtained from **1a,b**, and these two species are ascribed to the neutral monodentate NHC complexes **12a,b** and the corresponding chelating ionic complexes **13a,b**. In fact, they are in equilibrium in CD₂Cl₂ or CDCl₃. Addition of KPF₆ to an acetone solution of **12b** and **13b** completely shifted the equilibrium to the right side with anion exchange, and **14b** was isolated in 95% yield. Complex **14a** could be synthesized analogously. The CH₂ protons in **14a,b** are diastereotopic; the carbene C atoms resonate at δ 164.8 and 161.7, respectively, and they are more shielded than those in the iridium(I) cyclooctadiene complexes.

Equilibrium between 12b and 13b. The equilibrium between **12b** and **13b** has been studied in detail by NMR spectroscopy

(13) (a) Hanasaka, F.; Fujita, K.; Yamaguchi, R. *Organometallics* **2004**, *23*, 1490–1492. (b) Corberan, R.; Sanau, M.; Peris, E. *J. Am. Chem. Soc.* **2006**, *128*, 3974–3979. (c) Wang, X.; Chen, H.; Li, X. *Organometallics* **2007**, *26*, 4684–4687.

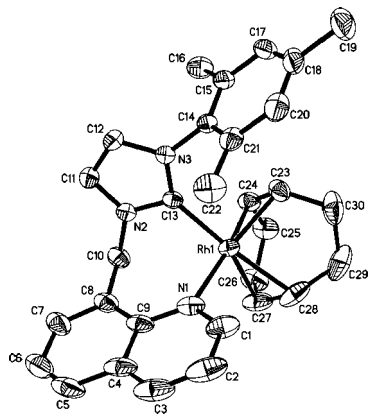


Figure 1. Molecular structure of **4** with thermal ellipsoids drawn at the 50% probability level. Hydrogen atoms and the anion are omitted for clarity. Selected lengths (Å) and angles (deg): Rh(1)–C(13), 2.0288(19); Rh(1)–N(1), 2.1677(18); Rh(1)–C(23), 2.124(2); Rh(1)–C(24), 2.135(2); Rh(1)–C(27), 2.183(2); Rh(1)–C(28), 2.217(2); C(23)–C(24), 1.401(3); C(27)–C(28), 1.380(4); N(1)–Rh(1)–C(13), 86.41(7); N(2)–C(13)–N(3), 104.37(16).

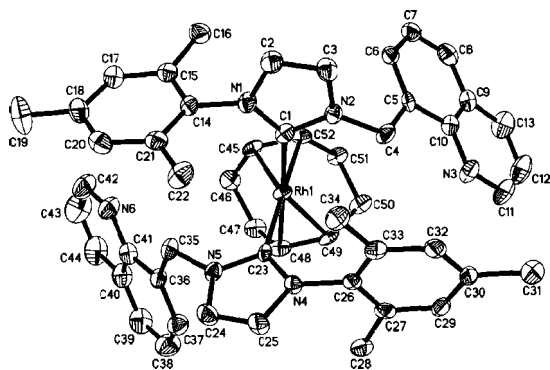


Figure 2. Molecular structure of **5** with thermal ellipsoids drawn at the 50% probability level. Hydrogen atoms and the anion are omitted for clarity. Selected lengths (Å) and angles (deg): Rh(1)–C(1), 2.091(5); Rh(1)–C(23), 2.072(5); Rh(1)–C(45), 2.165(5); Rh(1)–C(48), 2.218(5); Rh(1)–C(49), 2.175(5); Rh(1)–C(52), 2.226(5); C(45)–C(52), 1.372(8); C(48)–C(49), 1.385(8); C(1)–Rh(1)–C(23), 93.94(18); N(1)–C(1)–N(2), 104.3(4); N(4)–C(23)–N(5), 103.6(4).

Table 2. Measurement of the K_{eq} Values between **12b** and **13b** at Different Temperatures

T (K)	[12b] (M)	[13b], [Cl [−]] (M)	K_{eq} ([13b] ² /[12b])
297.1	0.022 41	0.015 35	0.0105
303.1	0.021 17	0.017 16	0.0139
313.1	0.018 85	0.019 22	0.0196
318.1	0.017 50	0.020 84	0.0248
323.1	0.016 44	0.022 24	0.0301
328.1	0.015 22	0.023 51	0.0363

in CDCl₃. Addition of tetra-*n*-butylammonium chloride to a mixture of **12b** and **13b** led to a decrease in the signal intensity of one component, unambiguously ascribed to **13b**, and an increase in that of the other, which was ascribed to **12b**, on the basis of the common ion effect. The equilibrium constants at various temperatures were then measured with 1,3,5-trimethoxybenzene as an internal standard by ¹H NMR spectroscopy. These data are shown in Table 2, and the van't Hoff plot based on these data gives $\Delta H^\circ = 32.1 \text{ kJ mol}^{-1}$ and $\Delta S^\circ = 70.1 \text{ J mol}^{-1} \text{ K}^{-1}$ ($R^2 = 0.9979$). This intramolecular chloride substitution is endothermic, possibly due to the ring strain in combination with the charge separation in **13b**. The large positive value of

ΔS° is also consistent with the more disordered structure of complex **13b**.

X-ray Structures. Single crystals of **4** and **5** were obtained by layering their CH₂Cl₂ solutions with diethyl ether (Table 3). Complex **4** cocrystallized with 1 equiv. of ether and it has a square-planar geometry (Figure 1). The Rh–C_{carbene} distance (2.0288(19) Å) is within the normal range for rhodium–NHC complexes.^{10b,14} The seven-membered rhodacycle adopts a boat conformation and is highly twisted. Indicative of the ring strain, the imidazole and the pyridine rings are nearly perpendicular to each other and the rhodium atom is not positioned exactly along the C(1)–N(1)–C(9) bisector but is displaced away from the pyridine ring. The Rh–C(27) and Rh–C(28) distances are at least 0.05 Å longer than those of Rh–C(23) and Rh–C(24), undoubtedly due to the high trans effect of the NHC ligand. Complex **5** is also square planar in geometry and is nearly C₂ symmetrical in the solid state (Figure 2). The two Rh–C_{carbene} distances (2.072(5) and 2.091(5) Å) are similar and are at least 0.04 Å longer than that in complex **4**, possibly due to the increased steric bulk rendered by the introduction of the second NHC ligand or due to the cis effect of these NHC ligands. The two NHC rings offset each other by 78.79°, and each is nearly perpendicular to the rhodium coordination plane. The solution structure elucidated by NMR spectroscopy is consistent with the solid-state analysis, where the C₂-symmetrical solution structure should exist in the time average. For example, the number of resonance signals in the ¹³C NMR spectrum (26) is half of the total number of C atoms (52), suggestive of the C₂ symmetry.

Single crystals of **14a** were obtained by slow diffusion of diethyl ether into a CH₂Cl₂ solution, and 1/2 equiv of CH₂Cl₂ is cocrystallized. X-ray crystallography confirmed the proposed structure of complex **14a** (Figure 3). This seven-membered iridacycle also has a boat conformation and, suggestive of the ring strain and the steric bulk of the Mes group, there is strong in-plane distortion of the NHC ligand. Consequently, the iridium atom is not positioned along the bisector of the N(2)–C(21)–N(3), as indicated by the large difference between the N(2)–C(21)–Ir(1) (119.8(3)°) and the N(3)–C(21)–Ir(1) (136.0(3)°) angles.

Electrochemistry. Cyclic voltammograms (CVs) of compounds **4**–**11** were obtained at a scan rate of 0.1 V s^{−1} at a GC electrode in CH₂Cl₂ and are shown in Figure 4. The compounds were all able to undergo a one-electron-oxidation process with the anodic peak potential (E_p^{ox}) ranging from +0.1 to +0.7 V vs Fc/Fc⁺. For all such compounds, the peak current for the anodic reaction (i_p^{ox}) was greater than the cathodic peak current (i_p^{red}) detected when the scan direction was reversed. The large $i_p^{\text{ox}}/i_p^{\text{red}}$ ratio is caused by the chemical instability of the oxidized compounds, indicating that they undergo an EC mechanism (where E is an electron transfer and C is a chemical step) on the time scale of the experiment.

As the scan rate was increased toward 5 V s^{−1}, the $i_p^{\text{ox}}/i_p^{\text{red}}$ ratio became closer to unity, indicating that the chemical step could be outrun at intermediate voltammetric scan rates. Nevertheless, increasing the scan rate also resulted in the E_p^{ox} and E_p^{red} separation (ΔE_{pp}) increasing for all of the compounds, significantly more than could be accounted for by the effects of uncompensated solution resistance. The increase in ΔE_{pp} with increasing scan rate is illustrated in Figure 5a for compound **9**, which also shows the $i_p^{\text{ox}}/i_p^{\text{red}}$ ratio increasing with increasing scan rate. Therefore, it can be concluded that the compounds display relatively slow rates of heterogeneous electron transfer.

(14) Herrmann, W. A.; Schutz, J.; Frey, G. D.; Herdtweck, E. *Organometallics* **2006**, *25*, 2437–2448.

Table 3. Crystallographic Data for Complexes **4**, **5**, and **14a**

	4 ·Et ₂ O	5	14a ·0.5CH ₂ Cl ₂
empirical formula	C ₃₀ H ₃₃ F ₆ N ₃ PRh·Et ₂ O	C ₅₂ H ₅₄ F ₆ N ₆ PRh	C ₃₂ H ₃₆ ClF ₆ IrN ₃ P·0.5CH ₂ Cl ₂
mol wt	757.59	1010.89	877.72
radiation, λ(Å)		Mo Kα (monochromated), 0.710 73 Å	
T (K)		173(2)	
cryst syst	monoclinic	monoclinic	triclinic
space group	P2 ₁ /n	P2 ₁ /n	P-1
a (Å)	11.2937(3)	17.9389(6)	8.6792(4)
b (Å)	27.1335(8)	15.8145(7)	14.4528(6)
c (Å)	11.4634(3)	18.7496(5)	14.4654(6)
α (deg)	90	90	110.965(2)
β (deg)	105.052(1)	117.490(2)	95.119(1)
γ (deg)	90	90	92.420(1)
V (Å ³)	3392.29(16)	4718.6(3)	1682.27(13)
Z	4	4	2
D _{calcd} (g cm ⁻³)	1.483	1.423	1.773
μ (mm ⁻¹)	0.615	0.463	4.236
cryst size (mm)	0.30 × 0.20 × 0.20	0.25 × 0.15 × 0.10	0.30 × 0.25 × 0.15
total, unique no. of rflns	96 133, 10 259	35 106, 8205	30 719, 10 112
R _{int}	0.0412	0.0799	0.0246
no. of data, restraints, params	10 259, 0, 420	8205, 0, 602	10 112, 2, 429
R, R _w	0.0361, 0.0900	0.0664, 0.175	0.0370, 0.1053
GOF	1.068	1.027	1.101
min, max resid dens (e Å ⁻³)	-0.603, 0.842	-0.0909, 1.483	-3.04, 1.857

The effect is particularly pronounced on Pt surfaces, where the oxidation processes were shifted to more positive potentials (Figure 5b).

The slow heterogeneous electron transfer rates and the chemical instability of the oxidized states make it difficult to accurately calculate the formal one-electron -oxidation potentials. It can be observed in Figure 4 that the E_p^{ox} values for compounds **4** and **5** are more positive than those observed for the other compounds, which can be accounted for by their formal positive charge (**4** and **5** exist as cations), making them more difficult to oxidize. However, compound **11** also has a positive charge but is oxidized at a potential very similar to that of the closely related neutral compound **10**.

The i_p^{ox} values observed for compounds at the same concentration and scan rate were similar, suggesting that the oxidation process occurred by the same number of electrons (although the peak current relationship depends on the diffusion coefficient of the molecules and is complicated by the slow rates of heterogeneous electron transfer). Controlled-potential electrolysis and coulometry experiments conducted on compound **10** (the compound that appeared the most chemically reversible at slow scan rates) led to the transfer of 1.1 electrons per

molecule, supporting the notion that the oxidation processes all occur via one electron. Under electrolysis conditions the oxidized form of **10** was not long-lived, such that the starting material could not be regenerated when a reducing potential was applied.

Rh(I)-Catalyzed [3 + 2] Cycloaddition Reactions. Rhodium can mediate a variety of organic transformations, including hydroformylation,¹⁵ hydrosilylation,^{8b,16} hydroboration,¹⁷ cyclotrimerization,¹⁸ and asymmetric hydrogenation.¹⁹ In recent years, with the development of metal complexes containing N-heterocyclic carbenes, Rh(I)-NHC complexes have been

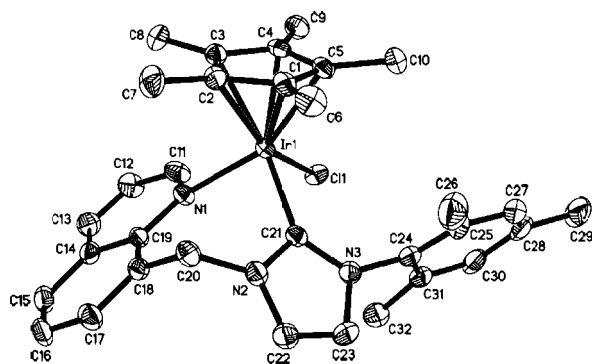


Figure 3. Molecular structure of **14a** with thermal ellipsoids drawn at the 50% probability level. Hydrogen atoms and the anion are omitted for clarity. Selected lengths (Å) and angles (deg): Ir(1)–C(21), 2.058(5); Ir(1)–Cl(1), 2.4098(10); Ir(1)–N(1), 2.190(4); N(1)–Ir(1)–C(21), 89.95(16); N(2)–C(21)–Ir(1), 119.8(3); N(3)–C(21)–Ir(1), 136.0(3); N(2)–C(21)–N(3), 104.2(4).

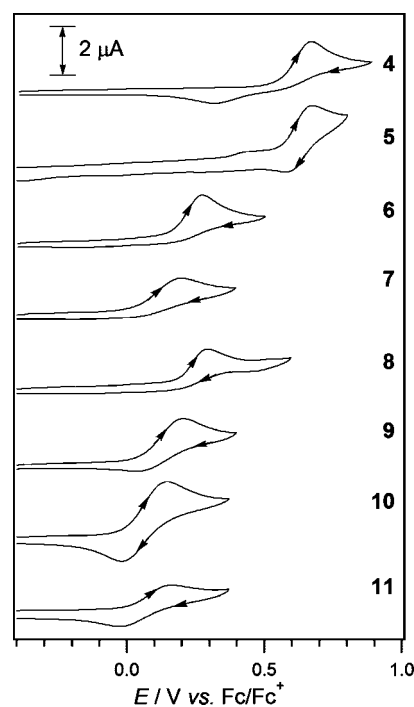


Figure 4. Cyclic voltammograms of 1 mM solutions of compounds **4**–**11** performed at a 1 mm diameter planar GC electrode in CH₂Cl₂ (containing 0.2 M Bu₄NPF₆) at a scan rate of 100 mV s⁻¹ at 20 ± 0.2 °C.

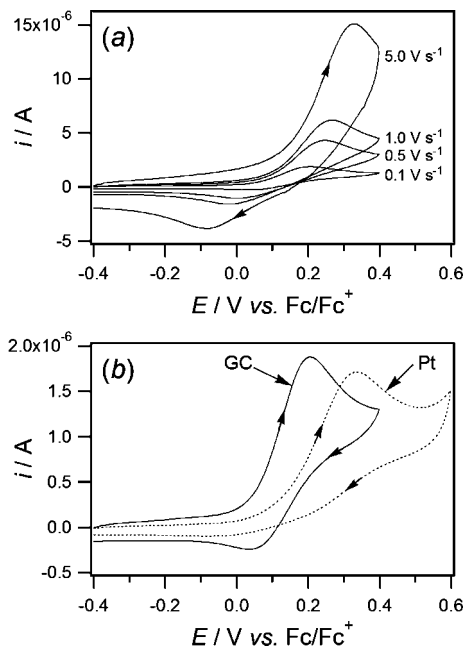
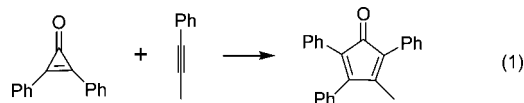


Figure 5. Cyclic voltammograms of a 1 mM solution of compound **9** performed at a 1 mm diameter planar electrode in CH_2Cl_2 (containing 0.2 M Bu_4NPF_6) at 20 ± 0.2 °C: (a) voltammograms recorded at variable scan rates at a GC electrode; (b) voltammograms recorded at a scan rate of 0.1 V s^{-1} at GC (solid line) and Pt (dashed line) electrodes.

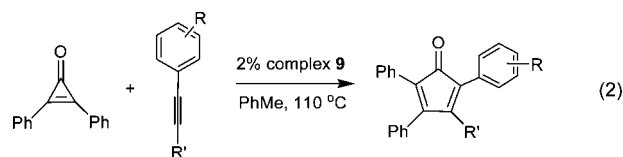
successfully applied to hydroformylation,²⁰ hydrosilylation,^{5a,21} intramolecular hydroamination,²² and carbocyclization.²³ However, to the best of our knowledge, there have been only two reports on cycloaddition reactions using well-characterized rhodium–NHC catalysts.²⁴

In 2006, Wender and co-workers reported that $[\text{RhCl}(\text{CO})_2]_2$ could catalyze the [3 + 2] cycloaddition of diphenylcyclopropanone and alkynes (eq 1).²⁵ In view of the high cost and sensitivity of $[\text{RhCl}(\text{CO})_2]_2$, we examined this reaction using



$\text{Rh}(\text{COD})(\text{NHC})\text{Cl}$ complexes as catalysts. Heating (110 °C) diphenylcyclopropanone and 1-phenyl-1-propyne in the presence of 5 mol % of compound **6** rapidly led to a dark purple solution, and the desired product was isolated in 77% yield. Other rhodium catalysts were then screened, and the results are displayed in Table 4. Complex **9**, which has an ⁱPr NHC wingtip group, shows the highest catalytic activity (entry 2, Table 4). Surprisingly, changing the wingtip group to a Mes, ^tBu, or ⁿBu group gave rise to significant drops of the catalytic activity in every case. The ionic rhodium carbene complexes **4** and **5** all showed poor activity for this reaction.

We then retained complex **9** to further study the scope of this catalytic reaction (eq 2), and the results are shown in Table 5. Electron-donating substituents in the aromatic ring favor this



reaction (entries 1 and 2, Table 5). Furthermore, catalyst **9** can also tolerate other functional groups such as a ketone (entry 5), an ester (entry 6), and a hydroxyl group (entry 7). Diphenylacetylene only gives 8% yield after 18 h at 110 °C (entry 8), and $o\text{-CH}_3(\text{C}_6\text{H}_4)\text{C}\equiv\text{CSiMe}_3$ failed to react (entry 9), which might be due to the steric hindrance. In addition, $\text{PhC}\equiv\text{CH}$ and $\text{MeO}_2\text{CC}\equiv\text{CO}_2\text{Me}$ failed to give any product under the same conditions, which is consistent with Wender's report.²⁵

Conclusions

A series of rhodium and iridium complexes of quinoline-tethered hemilabile N-heterocyclic carbenes (NHC[^]N) have been synthesized via either deprotonation of imidazolium salts or silver transmetalation. Deprotonation of imidazolium ions using ^tBuOK in the presence of $[\text{Rh}(\text{COD})\text{Cl}]_2$ afforded a mixture of chelating $[\text{Rh}(\text{COD})(\text{NHC}^{\wedge}\text{N})]^+$ and monodentate $[\text{Rh}(\text{COD})(\text{NHC})_2]^+$ complexes, while only the chelating complexes were obtained for the iridium analogues. Silver transmetalation of this type of carbene to $[\text{M}(\text{COD})\text{Cl}]_2$ ($\text{M} = \text{Rh}, \text{Ir}$) consistently afforded monodentate carbene complexes $\text{M}(\text{NHC})(\text{COD})\text{Cl}$, maintaining the pendant quinoline entity. Silver transmetalation of these carbenes to $(\text{Cp}^*\text{IrCl}_2)_2$ gave an equilibrium mixture of neutral $\text{Cp}^*\text{Ir}(\text{NHC})\text{Cl}_2$ and ionic $[\text{Cp}^*\text{Ir}(\text{NHC}^{\wedge}\text{N})\text{Cl}]\text{Cl}$ complexes. $\text{Rh}(\text{COD})(\text{NHC})\text{Cl}$ proved to be active in catalyzing the [3 + 2] cycloaddition reactions of diphenylcyclopropanone and internal alkynes. The carbene wingtip has significant effects on the catalytic activity, and the ⁱPr wingtip gives the highest activity among those screened. Crystal structures of metal complexes in each category have been reported.

Electrochemical experiments performed on compounds **4–11** indicate that all of them can undergo one-electron oxidation. The variable-scan-rate cyclic voltammetry experiments indicate that these compounds undergo relatively slow heterogeneous electron transfer and that the oxidized form of compound **9** is the most long-lived among those of compounds **6–9**. However, the oxidation potentials of these compounds appear to be very

(15) (a) Spencer, A. *J. Organomet. Chem.* **1980**, *194*, 113–123. (b) Kuil, M.; Soltner, T.; van Leeuwen, P. W. N. M.; Reek, J. N. H. *J. Am. Chem. Soc.* **2006**, *128*, 11344–11345.

(16) (a) Yao, S.; Meng, J.-C.; Siuzdak, G.; Finn, M. G. *J. Org. Chem.* **2003**, *68*, 2540–2546. (b) Sato, A.; Kinoshita, H.; Shinokubo, H.; Oshima, K. *Org. Lett.* **2004**, *6*, 2217–2219.

(17) (a) Luna, A. P.; Bonin, M.; Micouin, L.; Husson, H.-P. *J. Am. Chem. Soc.* **2002**, *124*, 12098–12099. (b) Kinder, R. E.; Widenhofer, R. A. *Org. Lett.* **2006**, *8*, 1967–1969. (c) Smith, S. M.; Thacker, N. C.; Takacs, J. M. *J. Am. Chem. Soc.* **2008**, *130*, 3734–3735.

(18) (a) Kinoshita, H.; Shinokubo, H.; Oshima, K. *J. Am. Chem. Soc.* **2003**, *125*, 7784–7785. (b) Tanaka, K.; Sagae, H.; Toyoda, K.; Noguchi, K.; Hirano, M. *J. Am. Chem. Soc.* **2007**, *129*, 1522–1523.

(19) (a) Hoge, G.; Wu, H.-P.; Kissel, W. S.; Pflum, D. A.; Greene, D. J.; Bao, J. *J. Am. Chem. Soc.* **2004**, *126*, 5966–5967. (b) Liu, Y.; Ding, K. *J. Am. Chem. Soc.* **2005**, *127*, 10488–10489.

(20) (a) Chen, A. C.; Ren, L.; Decken, A.; Crudden, C. M. *Organometallics* **2000**, *19*, 3459–3461. (b) Praetorius, J. M.; Kotyk, M. W.; Webb, J. D.; Wang, R.; Crudden, C. M. *Organometallics* **2007**, *26*, 1057–1061.

(21) (a) Park, K. H.; Kim, S. Y.; Son, S. U.; Chung, Y. K. *Eur. J. Org. Chem.* **2003**, 4341–4345. (b) Faller, J. W.; Fontaine, P. P. *Organometallics* **2006**, *25*, 5887–5893. (c) Özdemir, I.; Yiğit, M.; Yiğit, B.; Çetinkaya, B.; Çetinkaya, E. *J. Coord. Chem.* **2007**, *60*, 2377–2384.

(22) Field, L. D.; Messerle, B. A.; Vuong, K. Q.; Turner, P. *Organometallics* **2005**, *24*, 4241–4250.

(23) Evans, P. A.; Baum, E. W.; Fazal, A. N.; Pink, M. *Chem. Commun.* **2005**, 63–65.

(24) (a) Lee, S. I.; Park, S. Y.; Park, J. H.; Jung, I. G.; Choi, S. Y.; Chung, Y. K.; Lee, B. Y. *J. Org. Chem.* **2006**, *71*, 91–96. (b) Gómez, F. J.; Kamber, N. E.; Deschamps, N. M.; Cole, A. P.; Wender, P. A.; Waymouth, R. M. *Organometallics* **2007**, *26*, 4541–4545.

(25) Wender, P. A.; Paxton, T. J.; Williams, T. J. *J. Am. Chem. Soc.* **2006**, *128*, 14814–14815.

Table 4. Screening of Rhodium Catalysts for Eq 1

entry	catalyst (amt (mol %))	conditions	isolated yield (%)
1	6 (5)	18 h, 110 °C	77
2	9 (2)	2 h, 110 °C	84
3	7 (2)	6 h, 110 °C	24
4	8 (2)	6 h, 110 °C	12
5	4 (5)	18 h, 110 °C	27
6	5 (5)	18 h, 110 °C	–

Table 5. Substrate Scope of Eq 2

entry	R, R'	conditions	product	isolated yield (%)
1	<i>p</i> -CH ₃ , CH ₃ (15)	2 h, 110 °C	16	86
2	<i>p</i> -OCH ₃ , CH ₃ (17)	2 h, 110 °C	18	86
3	<i>p</i> -CF ₃ , CH ₃ (19)	6 h, 110 °C	20	68
4	<i>o</i> -Br, CH ₃ (21)	17 h, 110 °C	22	40
5	H, COCH ₃	18 h, 110 °C	23	80
6	H, COOEt	18 h, 110 °C	24	74
7	H, CH ₂ OH (25)	12 h, 110 °C	26	38
8	H, Ph	18 h, 110 °C	27	8
9	<i>o</i> -Me, Si(CH ₃) ₃ (28)	18 h, 110 °C	–	–

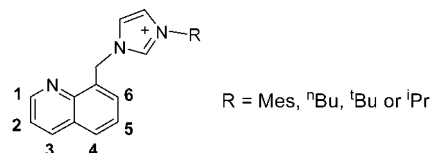
similar and it is not clear whether the oxidative behavior is important to the catalytic properties.

Experimental Section

General Procedures. All reactions were carried out at room temperature without exclusion of air unless otherwise noted. NMR spectra were recorded on Bruker Avance DPX 300 or Bruker AMX 400 MHz (¹H) and 75 or 100 MHz (¹³C), respectively, and were referenced to tetramethylsilane. Microanalyses were performed in the Elemental Analysis Laboratory of the Division of Chemistry and Biological Chemistry, Nanyang Technological University. X-ray crystallographic data were collected on a Bruker X8 APEX X-ray diffractometer.

Electrochemistry. Voltammetric experiments were conducted with a computer-controlled Eco Chemie Autolab III potentiostat with 1 mm diameter glassy-carbon (GC) and Pt-disk working electrodes. The miniature nonaqueous reference electrode was from Cypress Systems (EE008) and consisted of a silver wire inside a salt bridge containing 0.5 M Bu₄NPF₆ in CH₃CN. Fc/Fc⁺ (Fc = ferrocene) was measured as ~+0.4 V versus the Ag/Bu₄NPF₆/CH₃CN reference electrode. Accurate potentials were obtained for each compound by adding ferrocene during the final scans and recording the potential of the analyte directly against ferrocene using square-wave (SWV) and cyclic voltammetry (CV). The formal potential (*E*^o) measured for the oxidation of ferrocene (either the peak potential from SWV or the *E*_{1/2}^o from CV) was then digitally subtracted from the potential scale of each voltammogram. Voltammograms containing only the solvent and electrolyte showed no processes in the range over which the voltammetric scans were performed (±1 V vs Fc/Fc⁺), confirming that there were no interferences within the solvent/electrolyte. Coulometry experiments were performed in a divided controlled-potential electrolysis (CPE) cell separated with a porosity No. 5 (1.0–1.7 μm) sintered glass frit. The working and auxiliary electrodes were identically sized Pt-mesh plates symmetrically arranged with respect to each other with an Ag-wire reference electrode (isolated by a salt bridge) positioned to within 2 mm of the surface of the working electrode. The electrolysis cell was jacketed in a glass sleeve and cooled to 253 K using a Thermo Electron Neslab RTE 740 circulating bath with isopropyl alcohol. The volumes of both the working and auxiliary electrode compartments were approximately 10 mL each. The solution in the working electrode compartment was simultaneously deoxygenated and stirred using bubbles of argon gas. The number of electrons transferred during the bulk oxidation process was calculated from $N = Q/nF$, where N = no. of moles of starting compound, Q = charge (coulombs), n = no. of electrons, and F is the Faraday constant (96 485 C mol⁻¹).

General Procedure for the Synthesis of Imidazolium Salts 1a–d. A substituted imidazole was added to a solution of 8-(bromomethyl)quinoline²⁶ in acetonitrile, and the mixture was heated under reflux for 12–24 h. The solvent was then removed. Diethyl ether was added to the residue. The corresponding imidazolium salt was obtained as a solid or an oil.



Synthesis of 1a. 1-Mesitylimidazole (440 mg, 2.36 mmol) and 8-(bromomethyl)quinoline (500 mg, 2.25 mmol) were heated under reflux in MeCN (10 mL) for 16 h. A white solid was obtained following the workup, which was dried under vacuum to give an analytically pure white powder (912 mg, 99%). ¹H NMR (CDCl₃, 400 MHz): δ 10.40 (s, 1H, NCHN), 8.93 (dd, 1H, *J* = 4.2 and 1.5 Hz, H-1), 8.66 (d, 1H, *J* = 6.9 Hz), 8.22 (dd, 1H, *J* = 8.2 and 1.5 Hz, H-3), 8.16 (s, 1H, CH(imidazole)), 7.89 (d, 1H, *J* = 8.0 Hz), 7.61 (t, 1H, *J* = 7.4 Hz, H-5), 7.50 (dd, 1H, *J* = 8.3 and 4.2 Hz, H-2), 6.99 (s, 1H, CH(imidazole)), 6.95 (s, 2H, 2CH(mesityl)), 6.53 (s, 2H, CH₂(linker)), 2.30 (s, 3H, CH₃(mesityl)), 1.98 (s, 6H, CH₃(mesityl)). ¹³C{¹H} NMR (CDCl₃, 100 MHz): δ 150.2 (N–C(quinoline)), 146.3 (N–CH(quinoline)), 141.2, 138.0, 136.8, 134.3, 133.1, 131.7, 130.8, 130.0, 129.8, 128.5, 127.2, 124.1, 122.2 (imidazole), 121.7 (imidazole), 49.2 (CH₂(linker)), 21.1 (CH₃), 17.6 (2CH₃). Anal. Calcd for C₂₂H₂₂N₃Br (408.33): C, 64.71; H, 5.43; N, 10.29. Found: C, 64.46; H, 5.32; N, 10.37.

Synthesis of 1b. 1-*n*-Butylimidazole (409 mg, 3.30 mmol) and 8-(bromomethyl)quinoline (666 mg, 3.00 mmol) were heated under reflux in acetonitrile (10 mL) for 3 h. Product **1b** was obtained as an oil (1.0 g, 99%). ¹H NMR (CDCl₃, 400 MHz): δ 10.74 (s, 1H, NCHN), 8.98 (d, 1H, *J* = 2.8 Hz, H-1), 8.43 (d, 1H, *J* = 6.8 Hz), 8.21 (d, 1H, *J* = 8.1 Hz, H-3), 7.88 (d, 1H, *J* = 7.9 Hz), 7.78 (s, 1H, CH(imidazole)), 7.60 (t, 1H, *J* = 7.6 Hz, H-5), 7.50 (dd, 1H, *J* = 8.1 and 4.2 Hz, H-2), 7.20 (s, 1H, CH(imidazole)), 6.22 (s, 2H, CH₂(linker)), 4.28 (t, 2H, *J* = 7.4 Hz, NCH₂), 1.93–1.85 (m, 2H, NCH₂CH₂), 1.40–1.31 (m, 2H, NCH₂CH₂CH₂), 0.93 (t, 3H, *J* = 7.2 Hz, CH₃). ¹³C{¹H} NMR (CDCl₃, 100 MHz): δ 150.4 (N–C(quinoline)), 146.1 (N–CH(quinoline)), 137.4, 136.7, 132.5, 131.6, 130.0, 128.5, 127.0, 123.2, 121.8 (imidazole), 120.8 (imidazole), 49.8, 49.0 (CH₂(linker)), 32.1, 19.5, 13.4 (CH₃). Anal. Calcd for C₁₇H₂₀N₃Br (346.26): C, 58.97; H, 5.82; N, 12.14. Found: C, 58.78; H, 5.72; N, 12.23.

Synthesis of 1c. 1-*tert*-Butylimidazole (273 mg, 2.20 mmol) and 8-(bromomethyl)quinoline (444 mg, 2.00 mmol) were heated under reflux in MeCN (10 mL) for 3 h. **1c** was obtained as a white solid (680 mg, 98%). ¹H NMR (CDCl₃, 400 MHz): δ 10.88 (s, 1H, NCHN), 8.97–8.95 (m, 1H, H-1), 8.60 (d, 1H, *J* = 6.9 Hz), 8.21 (d, 1H, *J* = 8.2 Hz, H-3), 7.88–7.86 (m, 2H, CH(imidazole) + CH(quinoline)), 7.62 (t, 1H, *J* = 7.5 Hz, H-5), 7.50 (dd, 1H, *J* = 8.2 and 4.2 Hz, H-2), 7.29 (s, 1H, CH(imidazole)), 6.31 (s, 2H, CH₂(linker)), 1.69 (s, 9H, C(CH₃)₃). ¹³C{¹H} NMR (CDCl₃, 100 MHz): δ 150.2 (N–C(quinoline)), 146.0 (N–CH(quinoline)), 136.6, 135.6, 132.7, 131.8, 129.7, 128.3, 126.9, 123.4, 121.6 (imidazole), 118.5 (imidazole), 60.1 (C(CH₃)₃), 48.5 (CH₂(linker)), 30.0 (C(CH₃)₃). Anal. Calcd for C₁₇H₂₀N₃Br (346.26): C, 58.97; H, 5.82; N, 12.14. Found: C, 58.69; H, 5.94; N, 12.17.

Synthesis of 1d. 1-Isopropylimidazole (363 mg, 3.30 mmol) and 8-(bromomethyl)quinoline (666 mg, 3.00 mmol) were heated under reflux in MeCN (10 mL) for 3 h. **1d** was obtained as a white solid (968 mg, 97%). ¹H NMR (CDCl₃, 400 MHz): δ 10.78 (s, 1H,

(26) Dwyer, A. N.; Grossel, M. C.; Horton, P. N. *Supramol. Chem.* **2004**, *16*, 405–410.

NCHN), 8.96 (d, 1H, $J = 4.0$ Hz, H-1), 8.45 (d, 1H, $J = 6.7$ Hz), 8.20 (d, 1H, $J = 8.0$ Hz, H-3), 7.86 (d, 1H, $J = 8.0$ Hz), 7.80 (s, 1H, CH(imidazole)), 7.58 (t, 1H, $J = 7.2$ Hz, H-5), 7.49 (dd, 1H, $J = 8.2$ and 4.2 Hz, H-2), 7.37 (s, 1H, CH(imidazole)), 6.22 (s, 2H, CH₂(linker)), 4.82–4.78 (m, 1H, CH(CH₃)₂), 1.58 (d, 6H, $J = 6.6$ Hz, 2CH₃). ¹³C{¹H} NMR (CDCl₃, 100 MHz): δ 150.3 (N–C(quinoline)), 145.9 (N–CH(quinoline)), 136.6, 135.8, 132.2, 131.6, 129.8, 128.3, 126.7, 123.2, 121.7 (imidazole), 119.4 (imidazole), 53.0 (CH(CH₃)₂), 48.6 (CH₂(linker)), 23.0 (CH(CH₃)₂). Anal. Calcd for C₁₆H₁₈N₃Br (332.24): C, 57.84; H, 5.46; N, 12.65. Found: C, 57.50; H, 5.62; N, 12.77.

Synthesis of 2a. Imidazolium **1a** (650 mg, 1.59 mmol) was dissolved in acetone (10 mL), to which was added an acetone solution (5 mL) of KPF₆ (2.90 g, 15.9 mmol). The mixture was stirred for 3 h at room temperature. All the volatiles were then removed, followed by addition of CH₂Cl₂ (10 mL). Filtration gave a clear solution. **2a** was isolated as a white solid after the solvent was removed under vacuum (720 mg, 96%). ¹H NMR (CDCl₃, 400 MHz): δ 10.40 (s, 1H, NCHN), 8.93 (dd, 1H, $J = 4.2$ and 1.5 Hz, H-1), 8.66 (d, 1H, $J = 7.0$ Hz), 8.23 (dd, 1H, $J = 8.2$ and 1.4 Hz, H-3), 8.16 (s, 1H, CH(imidazole)), 7.88 (d, 1H, $J = 7.8$ Hz), 7.61 (t, 1H, $J = 7.5$ Hz, H-5), 7.48 (dd, 1H, $J = 8.3$ and 4.2 Hz, H-2), 6.99 (s, 1H, CH(imidazole)), 6.95 (s, 2H, 2CH(mesityl)), 6.53 (s, 2H, CH₂(linker)), 2.30 (s, 3H, CH₃(mesityl)), 1.98 (s, 6H, 2CH₃(mesityl)). ¹³C{¹H} NMR (CDCl₃, 100 MHz): δ 150.2 (N–C(quinoline)), 146.3 (N–CH(quinoline)), 141.2, 138.0, 136.8, 134.3, 133.1, 131.7, 130.8, 130.0, 129.8, 128.5, 127.2, 124.1, 122.2 (imidazole), 121.7 (imidazole), 49.2 (CH₂(linker)), 21.1 (CH₃), 17.6 (2CH₃). Anal. Calcd for C₂₂H₂₂N₃F₆P (473.39): C, 55.82; H, 4.68; N, 8.88. Found: C, 55.75; H, 4.77; N, 8.85.

Synthesis of 3. A THF solution of ^tBuOK (1.0 M, 0.26 mL) was added dropwise to a mixture of [Ir(COD)Cl]₂ (84 mg, 0.13 mmol) and THF (3 mL). After 30 min, a THF solution of **2a** (119 mg, 0.252 mmol) was added to this mixture and the mixture was stirred overnight. The solution was concentrated to ca. 1 mL and was chromatographed on silica gel with 10/1 CH₂Cl₂/acetone to give **3** as a yellow solid (146 mg, 76%). ¹H NMR (CDCl₃, 400 MHz): δ 9.38 (d, 1H, $J = 4.4$ Hz, H-1), 8.42 (d, 1H, $J = 8.0$ Hz, H-3), 8.33 (d, 1H, $J = 6.6$ Hz), 8.03–8.00 (m, 2H), 7.76 (t, 1H, $J = 7.6$ Hz, H-5), 7.63 (dd, 1H, $J = 8.1$ and 5.3 Hz, H-2), 7.50 (d, 1H, $J = 1.7$ Hz, CH(imidazole)), 6.97 (m, 2H, diastereotopic CH₂(linker) + CH(aromatic)), 6.61 (d, 1H, $J = 1.7$ Hz, CH(imidazole)), 5.90 (d, 1H, $J = 15.0$ Hz, diastereotopic CH₂(linker)), 4.15–4.12 (m, 1H, CH(COD)), 3.79–3.71 (m, 2H, 2CH(COD)), 3.48–3.43 (m, 1H, CH(COD)), 2.43–2.27 (m + s, 5H, CH₂(COD) + CH₃(mesityl)), 2.10–1.99 (m, 4H, 2CH₂(COD)), 1.95 (s, 3H, CH₃(mesityl)), 1.61 (s, 3H, CH₃(mesityl)), 1.38–1.28 (m, 2H, CH₂(COD)). ¹³C{¹H} NMR (CDCl₃, 100 MHz): δ 172.8 (carbene), 153.5, 145.6, 140.4, 139.6, 135.9, 134.91, 134.86, 134.2, 131.8, 131.5, 130.3, 129.4, 129.1, 128.4, 123.3, 121.6 (imidazole), 121.5 (imidazole) 85.0 (CH(COD)), 83.6 (CH(COD)), 63.9 (CH(COD)), 60.5 (CH(COD)), 53.6 (CH₂(linker)), 36.4 (CH₂(COD)), 33.1 (CH₂(COD)), 29.4 (CH₂(COD)), 26.5 (CH₂(COD)), 21.1 (CH₃(mesityl)), 17.8 (CH₃(mesityl)), 17.6 (CH₃(mesityl)). Anal. Calcd for C₃₀H₃₃F₆IrN₃P (772.78): C, 46.63; H, 4.30; N, 5.44. Found: C, 46.23; H, 4.45; N, 5.29.

Synthesis of 4 and 5. A THF solution of ^tBuOK (1.0 M, 0.25 mL) was added dropwise to a stirred suspension of imidazolium salt **2a** (118 mg, 0.250 mmol) in dry THF at room temperature. After the mixture was stirred for 30 min, [Rh(COD)Cl]₂ (62 mg, 0.13 mmol) was added in one portion. The reaction mixture was stirred overnight. Removal of the solvent gave a residue, which was chromatographed on silica gel with 25/1 CH₂Cl₂/acetone to give the yellow solid products **4** (88 mg, 65%) and **5** (22 mg, 10%).

Compound 4. ¹H NMR (CDCl₃, 400 MHz): δ 9.43 (d, 1H, $J = 4.7$ Hz, H-1), 8.54 (d, 1H, $J = 14.7$ Hz, diastereotopic CH₂(linker)), 8.40 (d, 1H, $J = 8.1$ Hz, H-3), 8.33 (d, 1H, $J = 6.9$ Hz), 7.98 (d,

1H, $J = 8.2$ Hz), 7.74 (t, 1H, $J = 7.4$ Hz, H-5), 7.63 (dd, 1H, $J = 8.2$ and 5.1 Hz, H-2), 7.45 (d, 1H, $J = 1.9$ Hz, CH(imidazole)), 7.08 (s, 1H, CH(mesityl)), 6.99 (s, 1H, CH(mesityl)), 6.62 (d, 1H, $J = 1.8$ Hz, CH(imidazole)), 5.86 (d, 1H, $J = 14.7$ Hz, diastereotopic CH₂(linker)), 4.61–4.58 (m, 1H, CH(COD)), 4.01–3.98 (m, 2H, CH(COD)), 3.81–3.79 (m, 1H, CH(COD)), 2.75–2.65 (m, 1H), 2.40 (s, 3H, CH₃(mesityl)), 2.38–2.11 (m, 6H, CH₂(COD)), 1.91 (s, 3H, CH₃(mesityl)), 1.71–1.64 (s + m, 4H). ¹³C{¹H} NMR (CDCl₃, 100 MHz): δ 175.4 (d, $J_{C-Rh} = 51.9$ Hz, C(NCN)), 153.2, 145.6, 140.1, 139.5, 135.1, 134.9, 134.7, 134.4, 131.3, 130.9, 130.8, 129.5, 129.1, 128.1, 123.8, 121.4, 121.3, 98.4 (d, $J_{C-Rh} = 7.6$ Hz, CH(COD)), 73.8 (d, $J_{C-Rh} = 13.2$ Hz, CH(COD)), 53.4 (CH₂(linker)), 35.3 (CH₂(COD)), 31.7 (CH₂(COD)), 29.2 (CH₂(COD)), 26.3 (CH₂(COD)), 21.1 (CH₃(mesityl)), 17.9 (CH₃(mesityl)), 17.6 (CH₃(mesityl)). Anal. Calcd for C₃₀H₃₃F₆N₃PRh · C₄H₁₀O: C, 53.90; H, 5.72; N, 5.55. Found: C, 53.43; H, 5.91; N, 5.62.

Compound 5. ¹H NMR (CDCl₃, 400 MHz): δ 8.86 (dd, 2H, $J = 4.1$ and 1.5 Hz, H-1), 8.20 (dd, 2H, $J = 8.2$ and 1.3 Hz, H-3), 7.83 (d, 2H, $J = 8.3$ Hz), 7.56–7.49 (m, 4H, H-5 + H-2), 7.26–7.22 (m, 8H, overlapping with solvent residue), 7.12 (d, 2H, $J = 17.1$ Hz, diastereotopic CH₂(linker)), 6.94 (d, 2H, $J = 1.6$ Hz, CH(imidazole)), 5.33 (d, 2H, $J = 16.9$ Hz, diastereotopic CH₂(linker)), 5.01 (br, 2H, 2CH(COD)), 3.61–3.56 (m, 2H, 2CH(COD)), 2.54 (s, 6H, 2CH₃(mesityl)), 1.95 (s, 6H, 2CH₃(mesityl)), 1.70 (s, 6H, 2CH₃(mesityl)), 1.59–1.56 (m, 4H, 2CH₂(COD)), 1.02–0.97 (m, 2H, CH₂(COD)), 0.65–0.60 (m, 2H, CH₂(COD)). ¹³C{¹H} NMR (CDCl₃, 100 MHz): δ 183.0 (d, $J_{C-Rh} = 54.2$ Hz, C(NCN)), 149.7, 145.7, 140.2, 136.3, 135.6, 135.5, 135.1, 135.0, 130.0, 129.6, 128.2, 128.1, 126.4, 126.3, 124.6, 123.2, 121.9, 92.6 (d, $J_{C-Rh} = 9.1$ Hz, CH(COD)), 83.3 (d, $J_{C-Rh} = 7.0$ Hz, CH(COD)), 52.3 (CH₂(linker)), 33.9 (CH₂(COD)), 26.2 (CH₂(COD)), 21.4 (CH₃), 17.75 (CH₃), 17.72 (CH₃). Anal. Calcd for C₅₂H₅₄F₆N₃PRh (1010.90): C, 61.78; H, 5.38; N, 8.31. Found: C, 61.70; H, 5.42; N, 8.27.

Synthesis of 6. Ag₂O (60 mg, 0.26 mmol) was added to a CH₂Cl₂ solution of complex **1a** (204 mg, 0.500 mmol), and this mixture was stirred for 1 h in the dark. Filtration of this mixture gave a clear solution, to which was added [Rh(COD)Cl]₂ (123 mg, 0.250 mmol) in one portion. The mixture was stirred for another 1 h. After filtration, the solvent was removed and the residue was washed with hexane twice to give **6** as a yellow solid product (278 mg, 97%). ¹H NMR (CDCl₃, 400 MHz): δ 8.98 (dd, 1H, $J = 4.0$ and 1.2 Hz, H-1), 8.23–8.17 (m, 2H), 7.85 (d, 1H, $J = 8.0$ Hz), 7.60 (t, 1H, $J = 7.7$ Hz, H-5), 7.47 (dd, 1H, $J = 8.2$ and 4.1 Hz, H-2), 7.10 (s, 1H), 7.03 (s, 1H), 6.95 (d, 1H, $J = 14.3$ Hz, diastereotopic CH₂(linker)), 6.91 (s, 1H), 6.65 (d, 1H, $J = 1.5$ Hz, CH(imidazole)), 6.38 (d, 1H, $J = 14.2$ Hz, diastereotopic CH₂(linker)), 4.92–4.83 (m, 2H, 2CH(COD)), 3.68 (br, 1H, CH(COD)), 3.05 (br, 1H, CH(COD)), 2.49 (s, 3H), 2.38 (s, 3H), 2.28–2.24 (m, 1H, CH₂(COD)), 2.18–2.09 (m, 1H, CH₂(COD)), 2.09–1.96 (m, 1H, CH₂(COD)), 1.82–1.67 (s + m, 6H, CH₃(mesityl) + CH₂(COD)), 1.56–1.48 (m, 2H, CH₂(COD)). ¹³C{¹H} NMR (CDCl₃, 100 MHz): δ 182.4 (d, $J_{C-Rh} = 49.7$ Hz, C(NCN)), 149.9, 146.7, 138.5, 137.2, 136.4, 135.2, 134.4, 131.3, 129.6, 128.4, 128.1, 126.6, 122.8, 121.6, 121.4, 96.8 (br, m, CH(COD)), 68.7 (br, CH(COD)), 67.6 (br, CH(COD)), 51.1 (CH₂(linker)), 33.8 (CH₂(COD)), 31.6 (CH₂(COD)), 29.2 (CH₂(COD)), 28.1 (CH₂(COD)), 21.1 (CH₃), 19.9 (CH₃), 17.8 (CH₃). Anal. Calcd for C₃₀H₃₃ClN₃Rh (573.96): C, 62.78; H, 5.80; N, 7.32. Found: C, 62.38; H, 5.87; N, 7.23.

The same procedure for complex **6** was followed in the preparation of complexes **7–9**. Complex **7** (yield 94%). ¹H NMR (CDCl₃, 400 MHz): δ 8.97 (dd, 1H, $J = 4.1$ and 2.6 Hz, H-1), 8.21 (dd, 1H, $J = 8.4$ and 1.4 Hz, H-3), 7.97 (d, 1H, $J = 7.0$ Hz), 7.80 (d, 1H, $J = 8.0$ Hz), 7.55 (t, 1H, $J = 7.6$ Hz, H-5), 7.46 (dd, 1H, $J = 8.3$ and 4.2 Hz, H-2), 6.81 (s, 1H, CH(imidazole)), 6.77 (s, 1H, CH(imidazole)), 6.57 (d, 1H, $J = 14.6$ Hz, diastereotopic

CH₂(linker)), 6.40 (d, 1H, *J* = 14.6 Hz, diastereotopic CH₂(linker)), 5.05 (br, 2H, 2CH(COD)), 4.59–4.51 (m, 2H, NCH₂), 3.53 (br, 1H, CH(COD)), 3.36 (br, 1H, CH(COD)), 2.43–2.34 (m, 4H, 2CH₂(COD)), 2.07–1.88 (m, 6H, NCH₂CH₂ + 2CH₂(COD)), 1.58–1.49 (m, 2H, NCH₂CH₂CH₂), 1.05 (t, 3H, *J* = 7.3 Hz, CH₃). ¹³C{¹H} NMR (CDCl₃, 75 MHz): δ 181.7 (d, *J*_{C–Rh} = 50.1 Hz, C(NCN)), 149.8, 146.3, 136.4, 134.9, 131.0, 128.7, 128.2, 128.1, 126.9, 121.2, 120.1, 98.3 (d, *J*_{C–Rh} = 6.9 Hz, CH(COD)), 98.1 (d, *J*_{C–Rh} = 7.0 Hz, CH(COD)), 68.5 (d, *J*_{C–Rh} = 14.6 Hz, CH(COD)), 68.2 (d, *J*_{C–Rh} = 14.6 Hz, CH(COD)), 50.6 (CH₂(linker)), 49.6 (NCH₂), 33.0, 32.9, 30.9, 28.9, 28.0, 20.2, 13.9 (CH₃). Anal. Calcd for C₂₅H₃₁ClN₃Rh (511.89): C, 58.66; H, 6.10; N, 8.21. Found: C, 58.46; H, 6.07; N, 8.29.

Complex **8** (yield 94%). ¹H NMR (CDCl₃, 400 MHz): δ 8.99 (d, 1H, *J* = 2.8 Hz, H-1), 8.21 (d, 1H, *J* = 8.2 Hz, H-3), 8.07 (d, 1H, *J* = 6.9 Hz), 7.80 (d, 1H, *J* = 8.0 Hz), 7.55 (t, 1H, *J* = 7.6 Hz, H-5), 7.46 (dd, 1H, *J* = 8.2 and 4.1 Hz, H-2), 7.08 (d, 1H, *J* = 14.7 Hz, diastereotopic CH₂(linker)), 6.94 (s, 1H, CH(imidazole)), 6.83 (d, 1H, *J* = 14.3 Hz, diastereotopic CH₂(linker)), 6.77 (s, 1H, CH(imidazole)), 5.00 (br, 2H, CH(COD)), 3.62 (br, 1H, CH(COD)), 3.37 (br, 1H, CH(COD)), 2.46–2.39 (m, 4H, 2CH₂(COD)), 2.00–1.81 (s + m, 13H). ¹³C{¹H} NMR (CDCl₃, 100 MHz): δ 180.6 (d, *J*_{C–Rh} = 49.9 Hz, C(NCN)), 149.9, 146.3, 136.5, 135.0, 131.3, 128.2, 128.0, 127.1, 121.2, 120.5, 119.7, 96.5 (d, *J*_{C–Rh} = 7.5 Hz, CH(COD)), 94.2 (d, *J*_{C–Rh} = 7.2 Hz, CH(COD)), 70.6 (d, *J*_{C–Rh} = 15.0 Hz, CH(COD)), 67.2 (d, *J*_{C–Rh} = 14.3 Hz, CH(COD)), 58.3 (C(CH₃)₃), 51.2 (CH₂(linker)), 33.3 (CH₂(COD)), 32.4 (C(CH₃)₃), 31.9 (CH₂(COD)), 29.4 (CH₂(COD)), 28.4 (CH₂(COD)). Anal. Calcd for C₂₅H₃₁ClN₃Rh (511.89): C, 58.66; H, 6.10; N, 8.21. Found: C, 58.39; H, 6.07; N, 8.26.

Complex **9** (yield 95%). ¹H NMR (CDCl₃, 400 MHz): δ 8.98 (dd, 1H, *J* = 4.2 and 1.7 Hz, H-1), 8.21 (dd, 1H, *J* = 8.2 and 1.6 Hz, H-3), 7.96 (d, 1H, *J* = 6.8 Hz), 7.80 (d, 1H, *J* = 8.2 Hz), 7.55 (t, 1H, *J* = 7.9 Hz, H-5), 7.46 (dd, 1H, *J* = 8.2 and 4.2 Hz, H-2), 6.85 (s, 1H, CH(imidazole)), 6.80 (s, 1H, CH(imidazole)), 6.57 (d, 1H, *J* = 14.6 Hz, diastereotopic CH₂(linker)), 6.40 (d, 1H, *J* = 14.8 Hz, diastereotopic CH₂(linker)), 5.88–5.81 (m, 1H, CH(CH₃)₂), 5.10 (br, 1H, CH(COD)), 5.00 (br, 1H, CH(COD)), 3.50 (br, 2H, CH(COD)), 2.50–2.30 (m, 4H, 2CH₂(COD)), 2.01–1.88 (m, 4H, 2CH₂(COD)), 1.51 (d, 3H, *J* = 6.0 Hz, CH₃), 1.49 (d, 3H, *J* = 6.0 Hz, CH₃). ¹³C{¹H} NMR (CDCl₃, 100 MHz): δ 181.4 (d, *J*_{C–Rh} = 52.5 Hz, C(NCN)), 149.8, 146.3, 136.5, 134.9, 130.9, 128.2, 128.1, 126.9, 121.6, 121.3, 116.4, 98.5 (d, *J*_{C–Rh} = 6.3 Hz, CH(COD)), 97.8 (br, CH(COD)), 68.3 (d, *J*_{C–Rh} = 13.9 Hz, CH(COD)), 67.9 (d, *J*_{C–Rh} = 15.5 Hz, CH(COD)), 52.5 (CH₂(linker)), 49.6 (CH(CH₃)₂), 33.5 (CH₂(COD)), 32.3 (CH₂(COD)), 29.4 (CH₂(COD)), 28.4 (CH₂(COD)), 23.3 (CH(CH₃)₂, accidentally equivalent). Anal. Calcd for C₂₄H₂₉ClN₃Rh (497.87): C, 57.90; H, 5.87; N, 8.44. Found: C, 57.78; H, 5.93; N, 8.36.

Synthesis of 10. The synthetic method for complex **6** was followed to prepare complex **10**, except that [Ir(COD)Cl]₂ was used (yield 95%). ¹H NMR (CDCl₃, 400 MHz): δ 8.97–8.96 (m, 1H, H-1), 8.18 (d, 1H, *J* = 8.4 Hz), 7.94 (d, 1H, *J* = 7.1 Hz), 7.78 (d, 1H, *J* = 8.1 Hz), 7.54 (t, 1H, *J* = 7.6 Hz, H-5), 7.46 (dd, 1H, *J* = 8.2 and 4.2 Hz, H-2), 6.88 (d, 1H, *J* = 1.0 Hz, CH(imidazole)), 6.77 (s, 1H, CH(imidazole)), 6.44 (d, 1H, *J* = 14.6 Hz, diastereotopic CH₂(linker)), 6.27 (d, 1H, *J* = 14.6 Hz, diastereotopic CH₂(linker)), 4.62 (s, 2H, 2CH(COD)), 4.42–4.38 (m, 2H, NCH₂), 3.10 (br, 1H, CH(COD)), 2.99 (br, 1H, CH(COD)), 2.22–2.18 (m, 4H, 2CH₂(COD)), 2.03–1.73 (m, 6H, 2CH₂(COD) + NCH₂CH₂), 1.53–1.45 (m, 2H, NCH₂CH₂CH₂), 1.01 (t, 3H, *J* = 7.3, CH₃). ¹³C{¹H} NMR (CDCl₃, 100 MHz): δ 179.9 (carbene), 149.8, 146.3, 136.5, 134.8, 130.8, 128.2, 128.1, 126.8, 121.3, 121.1, 119.9, 84.1 (CH(COD)), 83.9 (CH(COD)), 51.9 (CH(COD)), 51.8 (CH(COD)), 50.3, 49.2, 33.7, 33.5, 33.0, 29.7, 29.5, 20.1 (NCH₂CH₂CH₂), 13.8 (CH₃). Anal. Calcd for C₂₅H₃₁ClIrN₃ (601.20): C, 49.94; H, 5.20; N, 6.99. Found: C, 49.75; H, 5.21; N, 6.93.

Synthesis of 11. Complex **11** was prepared from complex **10** by following the same method as for the synthesis of **2a** (yield 96%). ¹H NMR (CD₃CN, 300 MHz): δ 9.00 (dd, 1H, *J* = 4.2 and 1.7 Hz, H-1), 8.35 (dd, 1H, *J* = 8.3 and 1.6 Hz, H-3), 7.92 (d, 1H, *J* = 8.1 Hz), 7.66–7.53 (m, 3H), 7.10 (d, 1H, *J* = 1.9 Hz, CH(imidazole)), 7.08 (d, 1H, *J* = 2.0 Hz, CH(imidazole)), 6.53 (d, 1H, *J* = 15.5 Hz, diastereotopic CH₂(linker)), 6.08 (d, 1H, *J* = 15.6 Hz, diastereotopic CH₂(linker)), 4.51–4.23 (m, 4H, 2CH(COD) + NCH₂), 3.06 (br, 2H, 2CH(COD)), 2.21–2.03 (m, 4H, 2CH₂(COD)), 1.86–1.82 (m, 2H, CH₂(COD)), 1.69–1.61 (m, 2H, NCH₂CH₂), 1.50–1.40 (m, 4H, CH₂(COD) + NCH₂CH₂CH₂), 1.05 (t, 3H, *J* = 7.3 Hz, CH₃). ¹³C{¹H} NMR (CD₃CN, 75 MHz): δ 179.5 (carbene), 151.1, 146.8, 137.5, 136.4, 129.9, 129.2, 129.1, 127.3, 122.7, 122.6, 121.8, 83.7 (CH(COD)), 53.1 (br, CH(COD)), 50.9 (CH₂(linker)), 50.7 (NCH₂), 34.2, 34.0, 33.7, 30.2, 30.1, 20.6 (NCH₂CH₂CH₂), 14.1 (CH₃), 1.20 (septet, ¹J_{DC} = 20.7 Hz, CD₃CN–Ir). The resonance signal of CD₃CN–Ir overlaps with that of the solvent peak (δ 118.2). Anal. Calcd for C₂₅H₃₁F₆IrN₃P (710.71): C, 42.25; H, 4.40; N, 5.91. Found: C, 42.11; H, 4.47; N, 5.85.

Synthesis of a Mixture of 12b and 13b. Ag₂O (32 mg, 0.14 mmol) was added to a CH₂Cl₂ solution of imidazolium salt **1b** (93 mg, 0.27 mmol). The mixture was stirred for 1 h in the dark. After filtration, [IrCp*Cl₂]₂ (108 mg, 0.136 mmol) was added in one portion to the solution, and this mixture was stirred for another 1 h. The solvent was removed, and the residue was washed with hexane to give yellow solid products (141 mg, 97%). Compound **12b**: ¹H NMR (CDCl₃, 400 MHz) δ 8.94 (dd, 1H, *J* = 4.1 and 1.6 Hz, H-1), 8.23–8.21 (m, 2H), 7.83–7.81 (m, 1H), 7.58–7.54 (m, 1H), 7.48–7.45 (m, 1H), 6.88 (d, 1H, *J* = 2.1 Hz, CH(imidazole)), 6.66 (d, 1H, *J* = 2.0 Hz, CH(imidazole)), 6.48 (d, 1H, *J* = 14.2 Hz, CH₂(linker)), 6.18 (d, 1H, *J* = 14.0 Hz, CH₂(linker)), 4.73–4.66 (m, 1H, NCH₂), 3.96–3.88 (m, 1H, NCH₂), 1.68 (s, 15H, 5CH₃), 1.55–1.44 (m, 2H, NCH₂CH₂), 1.42–1.37 (m, 2H, NCH₂CH₂CH₂), 1.01–0.93 (m, 3H, CH₃). Compound **13b**: ¹H NMR (CDCl₃, 400 MHz): δ 9.60 (dd, 1H, *J* = 5.6 and 1.7 Hz, H-1), 8.85–8.83 (m, 1H), 8.50 (d, 1H, *J* = 1.9 Hz, CH(imidazole)), 8.32 (dd, 1H, *J* = 8.2 and 1.5 Hz, H-3), 7.92–7.90 (m, 1H), 7.74–7.70 (m, 1H), 7.41–7.38 (m, 1H), 6.98 (d, 1H, *J* = 2.0 Hz, CH(imidazole)), 6.41 (d, 1H, *J* = 14.0 Hz, CH₂(linker)), 6.00 (d, 1H, *J* = 14.2 Hz, CH₂(linker)), 4.38–4.31 (m, 1H, NCH₂), 3.87–3.80 (m, 1H, NCH₂), 2.07–1.99 (m, 1H, NCH₂CH₂), 1.87–1.79 (m, 1H, NCH₂CH₂), 1.61 (s, 15H, 5CH₃), 1.44–1.37 (m, 2H, NCH₂CH₂CH₂), 1.00–0.93 (m, 3H, CH₃). Anal. Calcd for C₂₇H₃₄Cl₂IrN₃ (663.70): C, 48.86; H, 5.16; N, 6.33. Found: C, 48.74; H, 5.13; N, 6.38.

Synthesis of 14a. The procedure for the synthesis of the mixture of **12b** and **13b** was followed to prepare **12a** and **13a**, but no attempt was made to disentangle them in the ¹H NMR spectrum, since almost each of the resonance signals is broadened to a certain extent. No further characterization of the **12a** and **13a** mixture was performed. Instead, a mixture of **12a** and **13a** (91 mg, 0.13 mmol) was dissolved in CH₂Cl₂, and KPF₆ (230 mg, 1.25 mmol) was added quickly. The mixture was stirred for 3 h. After filtration, the solvent was evaporated under vacuum to give **14a** as a yellow solid (99 mg, 95%). ¹H NMR (CDCl₃, 400 MHz): δ 9.71 (dd, 1H, *J* = 5.5 and 1.7 Hz, H-1), 8.33 (dd, 1H, *J* = 8.1 and 1.6 Hz, H-3), 8.25–8.23 (m, 1H), 8.01–7.97 (m, 1H), 7.72 (s, 2H, 2CH(mesityl)), 7.42–7.38 (m, 1H), 6.88 (s, 1H), 6.80 (s, 1H), 6.65 (d, 1H, *J* = 1.8 Hz, CH(imidazole)), 6.50 (d, 1H, *J* = 15.0 Hz, diastereotopic CH₂(linker)), 5.88 (d, 1H, *J* = 14.9 Hz, diastereotopic CH₂(linker)), 2.31 (s, 3H, CH₃(mesityl)), 2.08 (s, 3H, CH₃(mesityl)), 1.58 (s, 3H, CH₃(mesityl)), 1.45 (s, 15H, 5CH₃). ¹³C{¹H} NMR (CD₃CN, 100 MHz): δ 161.7 (carbene), 152.8, 145.7, 141.6, 139.1, 138.5, 136.3, 135.9, 132.9, 132.7, 130.9, 128.7, 128.5, 127.7, 126.2, 122.8, 122.0, 91.5 (C₅Me₅), 53.5 (CH₂(linker)), 21.2 (CH₃(mesityl)), 19.1 (CH₃(mesityl)), 18.6 (CH₃(mesityl)), 9.1 (C₅Me₅). Anal. Calcd for

C₃₂H₃₆ClF₆N₃PIr (835.28): C, 46.01; H, 4.34; N, 5.03. Found: C, 46.14; H, 4.58; N, 5.30.

Synthesis of 14b. The same method as for **14a** was followed to prepare **14b**. Yield: 95%. ¹H NMR (CD₃CN, 400 MHz): δ 9.59 (d, 1H, *J* = 4.7 Hz, H-1), 8.50 (dd, 1H, *J* = 8.2 and 1.5 Hz, H-3), 8.07–8.01 (m, 2H), 7.70–7.66 (m, 1H), 7.59–7.52 (m, 2H), 7.26 (d, 1H, *J* = 2.0 Hz, CH(imidazole)), 6.14 (d, 1H, *J* = 14.4 Hz, diastereotopic CH₂(linker)), 5.26 (d, 1H, *J* = 14.5 Hz, diastereotopic CH₂(linker)), 4.38–4.31 (m, 1H, NCH₂), 3.93–3.86 (m, 1H, NCH₂), 1.98–1.96 (m, 2H, NCH₂CH₂), 1.61 (s, 15H, 5CH₃), 1.45–1.29 (m, 2H, NCH₂CH₂CH₂), 0.92 (t, 3H, *J* = 7.4 Hz, CH₃). ¹³C{¹H} NMR (CD₃CN, 100 MHz): δ 164.8 (carbene), 155.6, 146.0, 141.7, 134.8, 132.4, 130.4, 129.7, 127.0, 123.4, 122.7, 121.4, 91.4 (C₅Me₅), 50.7 (CH₂(linker)), 49.8 (NCH₂), 33.2 (NCH₂CH₂), 19.6 (NCH₂CH₂CH₂), 13.1 (CH₃), 8.3 (C₅Me₅). Anal. Calcd for C₂₇H₃₄ClF₆N₃PIr (773.21): C, 41.94; H, 4.43; N, 5.43. Found: C, 41.68; H, 4.48; N, 5.24.

Catalytic [3 + 2] Coupling. A rhodium catalyst (2%) and diphenylcyclopropenone (1.5 equiv) were weighed into a 20 mL flask. Dry toluene (1 mL) and alkyne were added via syringe sequentially. The mixture was heated for 2–18 h at 110 °C (see Tables 4 and 5). Removal of volatiles gave a residue that was then purified by silica gel column chromatography using hexane and ether as eluents. The coupling product was isolated as a purple or red product. The identity of products **18**, **20**, **23**, and **27** has been confirmed by comparison with the reported NMR spectra.²⁵ Products **16**, **22**, **24**, and **26** are new compounds. Substrates **15**,²⁷ **17**,²⁷ **19**,²⁸ **21**,²⁹ **25**,³⁰ and **28**³¹ were prepared following reported methods.

Product **16**: yield 86%; ¹H NMR (CDCl₃, 300 MHz) δ 7.43–7.22 (m, 14H), 2.42 (s, 3H), 2.12 (s, 3H); ¹³C{¹H} NMR (CDCl₃, 75 MHz) δ 200.7 (CO), 154.7, 153.4, 137.3, 133.9, 130.8, 129.9, 129.5, 129.1, 128.7, 128.6, 128.54, 128.48, 128.0, 127.3, 125.7, 124.6, 21.4, 14.6; IR (film) 3017 (w), 2922 (w), 1709 (m), 1510 (w), 1443 (w), 1379 (w), 1298 (w), 1215 (m), 1113 (w), 993 (w), 846 (w), 756 (s), 669 (m) cm⁻¹; HRMS (EI) *m/z* calcd for C₂₅H₂₀O 336.1509, found 336.1495.

(27) Vassilikogiannakis, G.; Orfanopoulos, M. *Tetrahedron Lett.* **1997**, *38*, 4323–4326.

(28) Weiss, H. M.; Touchette, K. M.; Angell, S.; Khan, J. *Org. Biomol. Chem.* **2003**, *1*, 2152–2156.

(29) Odedra, A.; Wu, C.-J.; Pratap, T. B.; Huang, C.-W.; Ran, Y.-F.; Liu, R.-S. *J. Am. Chem. Soc.* **2005**, *127*, 3406–3412.

(30) Lian, J.-J.; Chen, P.-C.; Lin, Y.-P.; Ting, H.-C.; Liu, R.-S. *J. Am. Chem. Soc.* **2006**, *128*, 11372–11373.

(31) Che, C.-M.; Yu, W.-Y.; Chan, P.-M.; Cheng, W.-C.; Peng, S.-M.; Lau, K.-C.; Li, W.-K. *J. Am. Chem. Soc.* **2000**, *122*, 11380–11392.

Product **22**: yield 40%; ¹H NMR (CDCl₃, 400 MHz) δ 7.66 (d, 1H, *J* = 7.6 Hz), 7.41–7.29 (m, 6H), 7.24–7.19 (m, 7H), 1.92 (s, 3H); ¹³C{¹H} NMR (CDCl₃, 100 MHz) δ 199.2 (CO), 156.9, 153.2, 133.6, 133.0, 132.0, 130.6, 130.0, 129.4, 128.74, 128.70, 128.6, 128.0, 127.5, 127.2, 127.1, 125.1, 124.6, 15.1; IR (film) 3019 (w), 1713 (m), 1645 (w), 1442 (w), 1378 (w), 1298 (w), 1215 (m), 1028 (w), 928 (w), 768 (s), 752 (s), 669 (m) cm⁻¹; HRMS (EI) *m/z* calcd for C₂₄H₁₇BrO 400.0457, found 400.0453.

Product **24**: yield 74%; ¹H NMR (CDCl₃, 400 MHz) δ 7.57–7.56 (m, 2H), 7.43–7.21 (m, 13H), 4.16–4.10 (m, 2H), 1.02 (t, 3H, *J* = 7.1 Hz); ¹³C{¹H} NMR (CDCl₃, 100 MHz) δ 199.4 (CO), 165.7 (COOCH₂CH₃), 153.0, 144.9, 133.1, 130.2, 130.0, 129.5, 129.4, 129.3, 129.0, 128.6, 128.4, 128.2, 127.9, 124.5, 61.6 (COOCH₂CH₃), 13.7 (COOCH₂CH₃); IR (film) 3019 (w), 1717 (m), 1645 (w), 1494 (w), 1445 (w), 1373 (w), 1354 (w), 1215 (m), 1119 (w), 1018 (w), 760 (m), 694 (m) cm⁻¹; HRMS (EI) *m/z* calcd for C₂₆H₂₀O₃ 380.1407, found 380.1364.

Product **26**: yield 38%; ¹H NMR (CDCl₃, 400 MHz) δ 7.51–7.36 (m, 10H), 7.21 (br, 5H), 4.53 (d, 2H, *J* = 5.8 Hz), 1.40 (t, 1H, *J* = 5.8 Hz); ¹³C{¹H} NMR (CDCl₃, 100 MHz) δ 200.6 (CO), 154.5, 152.4, 133.8, 130.5, 130.3, 129.9, 129.8, 129.1, 129.0, 128.5, 128.33, 128.25, 128.1, 128.0, 127.5, 125.3, 56.6; IR (film) 3483 (w), 3019 (w), 1699 (w), 1494 (w), 1445 (w), 1352 (w), 1215 (s), 1113 (w), 1003 (w), 922 (w), 756 (m), 669 (m) cm⁻¹; HRMS (EI) *m/z* calcd for C₂₄H₁₈O₂ 338.1301, found 338.1295.

Crystallographic Analysis. X-ray-quality single crystals of complexes **4**, **5**, and **14a** were obtained by the slow diffusion of diethyl ether into their dichloromethane solutions. Complex **4** cocrystallized with 1 equiv of ether, and complex **14a** cocrystallized with 1/2 equiv of CH₂Cl₂. Crystal data were collected on a Bruker X8 Kappa CCD diffractometer at 173 K using graphite-monochromated Mo Kα radiation (λ = 0.710 73 Å). The APEX2 software suite (Bruker, 2005) was used for data acquisition, structure solution, and refinement. Absorption corrections were applied using SADABS. The structure was solved by direct methods and refined by full-matrix least-squares methods on *F*² using Xshell.

Acknowledgment. We thank the School of Physical and Mathematical Sciences, Nanyang Technological University, for financial support and the Johnson Matthey Co. for a loan of iridium and rhodium chloride. Dr. Yongxin Li is gratefully acknowledged for the X-ray crystallographic analyses.

Supporting Information Available: Tables, figures and CIF files giving crystal data of complexes **4**, **5**, and **14a**. This material is available free of charge via the Internet at <http://pubs.acs.org>.

OM800404Q